

Adaptive Quantization and Fast Error Resilient Entropy Coding for Image Transmission

R. Chandramouli, N. Ranganathan, and Shivaraman J. Ramadoss

Abstract— Recently, there has been an outburst of research in image and video compression for transmission over noisy channels. Channel matched source quantizer design has gained prominence. Further, the presence of variable length codes in compression standards like the JPEG and the MPEG has made the problem more interesting. Error resilient entropy coding (EREC) [20] has emerged as a new and effective method to combat catastrophic loss in the received signal due to burst and random errors. In this paper, we propose a new channel matched adaptive quantizer for JPEG image compression. A slow, frequency non-selective Rayleigh fading channel model is assumed. The optimal quantizer that matches the human visibility threshold and the channel bit error rate is derived. Further, a new fast error resilient entropy code (FEREC) that exploits the statistics of the JPEG compressed data is proposed. The proposed FEREC algorithm is shown to be almost twice as fast as EREC in encoding the data and hence the error resilience capability is also observed to be significantly better. On an average, a 5% decrease in the number of significantly corrupted received image blocks is observed with FEREC. Upto a 2 dB improvement in the peak signal to noise ratio of the received image is also achieved.

Keywords— JPEG, image compression, error resilient coding, fading, adaptive quantization.

I. INTRODUCTION

IMAGE transmission through band limited and high bit error rate fading communication channels, like the wireless mobile channels, requires good compression algorithms and error resilient coding techniques. Short fade intervals induce high bit error rates. As a result, high data frame errors occur. Shannon showed that source and channel coding can be fundamentally separated. The entropy rate reduction is done by the source encoder and the protection against channel errors by the channel encoder. However, the separation is justifiable only in the limit of an arbitrary encoding complexity. In practical systems, when the complexity and the delay are the main constraints the tandem source-channel coding is not optimal [1]. The source and channel encoders are dependent on each other. Combined source-channel coding for image coding has been studied in [2]. In [3], the problem of optimum quantizer design for signal transmission over noisy channels is studied. Zero-memory quantizers with smaller bit rates are shown to perform better than high rate quantizers for very noisy channels.

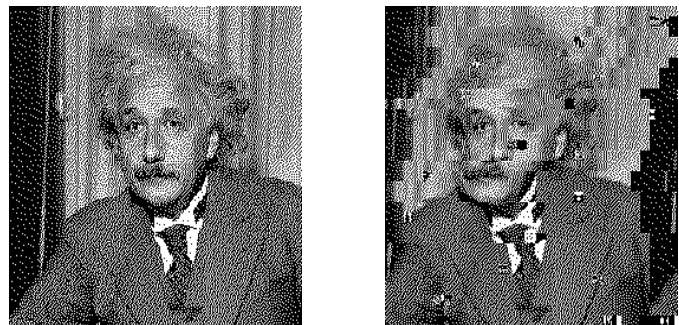
Manuscript received —

R. Chandramouli and N. Ranganathan are with the Center for Microelectronics Research, Department of Computer Science and Engineering, University of South Florida, Tampa, FL 33620, USA.

S.J. Ramadoss is with Digital Video Express, Herndon Parkway, Herndon, VA 20170, USA.

This work was done when S.J. Ramadoss was with the Department of Computer Science and Engineering, University of South Florida

Variable length codes are frequently used in low rate image coding systems. But these are known to be highly susceptible to channel errors. The critical bits need to be protected from channel errors in order to prevent the complete loss of a transmitted image. The synchronization of the decoder to the received bit stream could be lost due to bit errors. This leads to error propagation and the loss of the source symbols. The loss of a few blocks of symbols causes displacements in the received image. Error correcting codes that protect the critical bits from channel errors for image transmission are analyzed in [4]-[7]. Examples of the critical bits are the EOB (end of block) markers in JPEG compressed images and the most significant bit of a source symbol. An error in the most significant bit could cause higher degradation than a corrupted least significant bit. The loss of EOB due to errors leads to catastrophic error propagation as shown in Fig. 1. Therefore, the high priority bits need to be protected using channel coding or other methods. But the redundancy due to channel coding reduces the compression efficiency. Therefore, an optimal trade-off between the rate of the source coder and the channel coder is essential.



(a) original image

(b) error propagated image

Fig. 1. Effect of Error Propagation

Bit errors in variable length codes cause synchronization loss. In [9]-[13], synchronization codes to reduce this loss are discussed. But these codes have to be used infrequently in order to reduce the amount of redundancy. Also, the error propagation is limited only to the maximum separation between the sync words. Error propagation between different sets of variable length codes is not limited by the sync codes. However, most of the compression algorithms use different types of variable length codes.

Residual redundancy at the output of the source encoder in practical systems is due to the constraints on the encoder complexity and delay. This redundancy can be exploited at the decoder to perform forward error correction. In [14], the redundancy at the output of a DPCM coder has been used to correct channel errors. The redundancy in the adjacent vector quantizer indices is exploited in [15]. Adaptive interpolation in the spatial, temporal and frequency domains is used in [16] to recover damaged regions of the received video signal. Hybrid methods that incorporate many of these techniques for error protection, correction and error recovery of video signals for wireless channels are discussed in [17]-[18].

Error resilient coding reduces the redundancy due to channel coding and yet protects against error propagation. Recently, error resilient encoding for image and video transmission have been proposed in [19]-[20]. In [19], error resilient codes for subband image coding using vector quantization is studied. The positions and values of the *active* blocks of bits are encoded. A *comma* bit terminates each active block. But it requires a additional overhead of 0.6 bits over the entropy bound to code the position of each transmitted sample. This overhead is reduced in [20] using a bit re-organization algorithm. The variable lengths of data blocks (in bits) are placed into a fixed number of slots of equal size using an error resilient entropy coder (EREC). Initially, each block of data is placed into its corresponding slot either fully or partially. Then, a predefined offset sequence is used to search for empty slots to place the remaining bits of each block from the successive stages of the algorithm. This is done until all the bits are packed into one of the slots. The decoder synchronizes at the start of each block with minimal redundancy. EREC ensures that the bits at the beginning of each block is more immune to error propagation than those at the end. Therefore the error propagation is predominant only in the higher frequencies which are subjectively less important in images. Error resilient coding using bit re-organization has many advantages. A graceful degradation with increasing channel bit error rate is obtained. During burst errors, channel coding fails miserably if the depth of interleaving is insufficient. Deep interleaving causes unacceptable delays. On the other hand, error resilient entropy coding produces data that is corrupted only as long as the burst length with little or no additional delay and redundancy.

In this paper, we propose an adaptive quantizer and an efficient error resilient encoder for JPEG compressed image transmission over mobile wireless channels. A slow, frequency non-selective Rayleigh fading channel model is assumed. For very low bit error rates, the quantization table given in [21] for optimal human visual quality is used for compression. When the channel bit error rate changes, each entry in the quantization table is multiplied by an optimum factor M^* to control the bit rate at the output of the quantizer. The value of M^* is computed using a quadratic model that relates the average number of received image blocks in error and the channel bit error rate. The model parameters are estimated using extensive simulation and

statistical regression. M^* is computed for bit error rates ranging from 10^{-5} to 10^{-1} . The optimal quantizer for a particular channel bit error rate is designed using the corresponding value of M^* . In order to enhance the robustness of the adaptive system, we also propose a fast error resilient entropy coder (FEREC). Through simulations, it is shown that the encoder is twice as fast as EREC in packing the blocks of data into slots. As a result FEREC possesses superior error containment capabilities. The peak signal to noise ratio of the received image using FEREC is observed to be higher than that with EREC. A total number of 50 images are tested.

The paper is organized as follows. In Section II the baseline JPEG scheme used in our analysis is introduced and discussed briefly. Section III discusses the slow, frequency non-selective Rayleigh fading channel model. The bit error rate for BPSK transmission is derived as a function of the average signal to noise ratio. The fading channel simulator used in our experiments is discussed. The new adaptive quantization strategy is given in Section IV. The dependence of the quantizer on both the source and channel statistics is explained. The optimum quantization parameter M^* based on a new model is also derived. In Section V the proposed fast error resilient entropy coding method is given. The assumptions, observations and the algorithm are explained in detail. The working of the algorithm is illustrated using a simple example. The simulation results are given in Section VI. The advantages of the proposed adaptive quantization and the fast error resilient coder are supported through simulations. The assumptions used to design the fast error resilient encoder are also validated. Finally, conclusions and future work are discussed in Section VII.

II. THE BASELINE JPEG

The JPEG compression standard is widely used for still image compression [21]. The input image, X , is partitioned into $N \times N$ sub-blocks followed by the 2-D discrete cosine transform (DCT) for each sub-block. DCT reduces the inherent redundancy in the signal. The quantization of the DCT coefficients controls the achieved compression ratio. The DC coefficient has higher energy than the AC coefficients. Therefore, most of the AC coefficients are quantized to zero. Each DCT coefficient is divided by the corresponding quantization factor in the quantization table and truncated to an integer value. Dequantization is the inverse process. The quantization table in JPEG is designed using criteria based on the visibility threshold values for the DCT basis functions. Table I gives the visibility threshold values of the quantizer for a 8×8 sub-block of an image [21]. It is clear from the table that the DC and the lower frequency AC coefficients are finely quantized and the higher frequency AC coefficients are coarsely quantized. This is because, the energy of the DCT coefficients are concentrated mostly in the lower frequency coefficients. The quantization error is controlled by the quantization threshold values. The quantized coefficients are then zig-zag scanned, run-length and Huffman encoded

16	11	10	16	24	40	51	61
12	12	14	19	26	58	60	55
14	13	16	24	40	57	69	56
14	17	22	29	51	87	80	62
18	22	37	56	68	109	103	77
24	35	55	64	81	104	113	92
49	64	78	87	103	121	120	101
72	92	95	98	112	100	103	99

TABLE I
THE 8 × 8 JPEG QUANTIZATION TABLE

to get the final JPEG compressed image. Decompression is the exact reverse process.

III. FADING CHANNEL MODEL

Fading is caused due to randomly time-varying channel responses. If the signaling interval T is smaller than the coherence time of the channel, the channel attenuation and phase shift are approximately constant for that time interval. This leads to a slowly fading channel. When the signal bandwidth is much smaller than the coherence bandwidth of the channel, the channel is said to be frequency non-selective. That is, all the frequency components of the transmitted signal undergo the same attenuation and phase shift. In this study, we consider a slow, frequency non-selective Rayleigh fading channel with additive white Gaussian noise (AWGN). If the transmitted signal is $s(t)$, the received equivalent low pass signal in one signaling interval is

$$r(t) = \alpha e^{-j\phi} s(t) + z(t), \quad 0 \leq t \leq T \quad (1)$$

where α is the random channel attenuation and ϕ is the random phase shift. $z(t)$ represents the complex valued white Gaussian noise process. The probability density function of α and ϕ are given by

$$f(\alpha) = \frac{\alpha}{\sigma^2} e^{-\alpha^2/2\sigma^2}, \quad \alpha \geq 0 \quad (2)$$

$$g(\phi) = \frac{1}{2\pi}, \quad -\pi \leq \phi \leq \pi \quad (3)$$

Since the channel fading is slow, it can be assumed that the phase shift ϕ can be estimated from the received signal with very small error. Hence, coherent detection of the received signal is possible. If E_b denotes the energy per bit and N_0 is the noise power, then the conditional bit error probability for BPSK modulation is [1]

$$p_e(\gamma) = H(\sqrt{2\gamma}) \quad (4)$$

where $\gamma = \alpha^2 E_b / N_0$ is the signal to noise ratio for a fixed α and $H(x) = \frac{1}{\sqrt{2\pi}} \int_x^\infty e^{-t^2/2} dt$. Therefore, the probability of error for any attenuation α is given by

$$\begin{aligned} p_e &= \int_0^\infty p_e(\gamma) p(\gamma) d\gamma \\ &= \frac{1}{2} \left(1 - \sqrt{\frac{\bar{\gamma}}{1 + \bar{\gamma}}} \right) \end{aligned} \quad (5)$$

where $\bar{\gamma} = \frac{E_b}{N_0} \mathbf{E}(\alpha^2)$ is the average signal to noise ratio.

The fading channel simulator that we used is based on [23]. The set-up of the slow, frequency non-selective Rayleigh fading channel simulator used in our analysis is shown in Fig. 2. Two independent time-varying zero mean Gaussian noise sources are used for the in-phase (I -channel) and the quadrature phase channels (Q -channel). The Gaussian random variables g_1 and g_2 pass through a low pass filter that simulates the effects of the Doppler frequency shift. The filtered in-phase and the quadrature phase noise components, namely, $g_1^I(t)$ and $g_2^Q(t)$ together give the Rayleigh distributed fading channel.

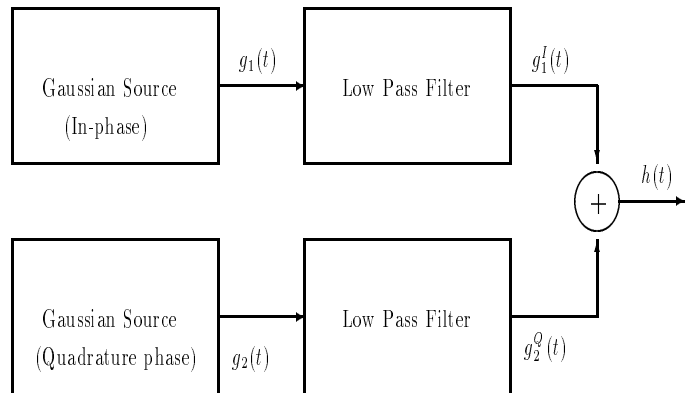


Fig. 2. Fading channel simulator

IV. ADAPTIVE QUANTIZER DESIGN

In this section, we briefly discuss the effects of the channel on the source quantizer. A new model to design the quantizer that matches the channel and the human visibility threshold level is proposed. The optimal quantizer is chosen based on the feedback from the receiver regarding the channel error rate.

A. Channel Effects on Source Quantizer

The errors in the reconstructed image sub-blocks are both due to the quantization and channel errors. At high bit error rates, p_e , a high rate quantizer is more sensitive to the channel errors. This causes many received blocks of data to be in error. But, we do not use any explicit channel coding in order to design a simple encoder and also avoid the additional redundancy. Also, we want to study purely the performance of the adaptive quantizer and FEREC. So, a lower rate quantizer is used by scaling up the entries of the quantization table by the quantizer factor, M , resulting in a fewer number of transmitted bits. This causes a reduction in the number of bit errors and hence the sub-block errors in the received signal. The number of blocks that are in error is a minimum for the optimal choice of M , namely, M^* . If the bit rate is reduced further then the quantization errors contribute significantly to the degradation in the received signal. Therefore, the number of

image sub-blocks in error increases again. If X denotes the source image, U is the quantized image and V is the received image, then the reconstruction error variance for a noisy channel is given by

$$\begin{aligned}
\sigma_{rec}^2 &= \mathbf{E} [X - V]^2 \\
&= \mathbf{E} [(X - U) + (U - V)]^2 \\
&= \mathbf{E} [X - U]^2 + \mathbf{E} [U - V]^2 + 2\mathbf{E} [(X - U)(U - V)] \\
&= \sigma_q^2 + \sigma_c^2 + 2\sigma_m^2
\end{aligned} \tag{6}$$

The quantities σ_q^2 , σ_c^2 and σ_m^2 denote the quantization, channel and the mutual error variance. The mutual error arises when the channel noise is mapped into reconstruction noise. This is equal to zero when the channel error probability is zero or a Max-quantizer is used [24]. But in practice, the contribution of σ_m^2 can be neglected for a small bit error probability [3], [24]. Therefore, the reconstructed error is approximately equal to the sum of the errors due to quantization and the channel. This leads to the *quantizer limited* and the *channel limited* conditions. But, in our simulations we have implicitly accounted for the mutual error variance. The quantization error variance is minimized using the optimal quantization values in Table I under error free channel conditions. When the channel is noisy, σ_c^2 is minimized by scaling the values of Table I by a proper choice of the quantizer parameter, M . Therefore, σ_{rec}^2 is minimized by the optimal choice of M . Thus, the optimal value M^* is a function of both σ_q^2 and σ_c^2 .

B. Q-C Modeling

Computing closed form expression for the optimal visibility quantization threshold values under noisy conditions is difficult. Therefore, an empirical method is used to compute the optimal quantizer. A $N \times N$ sub-block of the received image is deemed erroneous if the peak signal to noise ratio (PSNR) for that block given by

$$PSNR = 10 \log_{10} \left(\frac{255^2}{\frac{1}{N^2} \sum_{i=0}^{N-1} \sum_{j=0}^{N-1} (U(i, j) - V(i, j))^2} \right) \tag{7}$$

is less than 40 dB. We call the quantizer-channel error trade-off as the *Q-C curve*. It relates the number of image sub-blocks in error and the value of M . The parameters of the model are computed empirically using statistical regression for bit error rates ranging from 10^{-5} to 10^{-1} . The rate of the quantizer can be adapted to the channel bit error rate by suitably changing M . M^* is computed for each channel error rate. A look-up table is used for the adaptive quantization. To compute M^* , M is varied in steps of 0.1 and the average number of erroneously received image sub-blocks is computed for each p_e . The Q-C curves (non-smooth) when $N = 8$ averaged over 50 images compressed using the baseline JPEG configuration are shown in Fig. 3, 4 and 5.

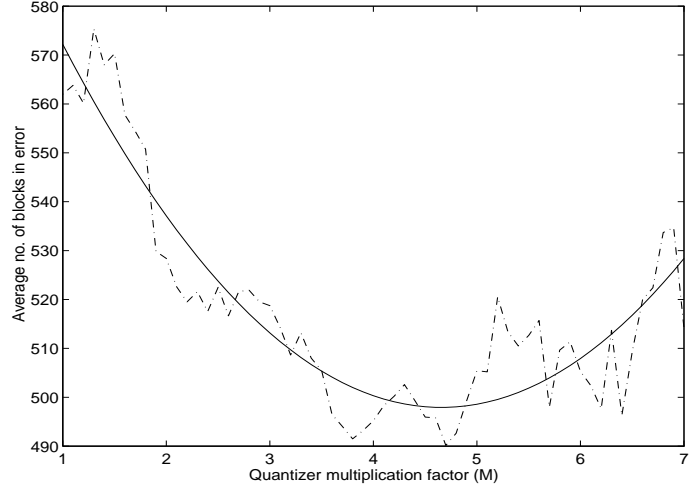


Fig. 3. Q-C curve for $p_e=10^{-1}$

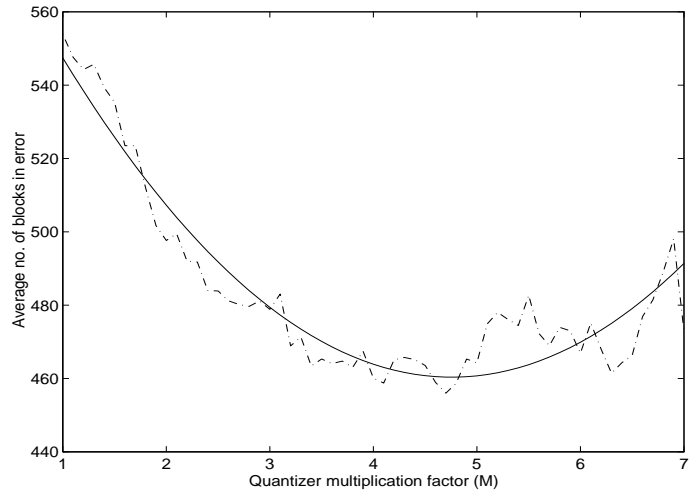


Fig. 4. Q-C curve for $p_e=10^{-2}$

As expected, for a high value of p_e , the channel errors dominate. But this effect diminishes with coarser quantization. For higher values of M , the quantization error dominates. For a fixed p_e the figures suggest that the Q-C curve can be modeled as

$$\begin{aligned}
B(M) &= a_0 + a_1 M + a_2 M^2 \\
&= a_2 \left[M - \left(-\frac{a_1}{2a_2} \right) \right]^2 + \frac{4a_2 a_0 - a_1^2}{4a_2} \tag{8}
\end{aligned}$$

B is the average number of received image sub-blocks that are in error and a_i , $i = 0, 1, 2$ are the unknown parameters of the model. We use statistical regression to estimate the a_i 's. It is clear from Fig. 3-Fig. 5 that the model fits the actual Q-C curve very well. It is possible that the modeling error could be large when the channel behaves abnormally. But we have found through experiments that the second

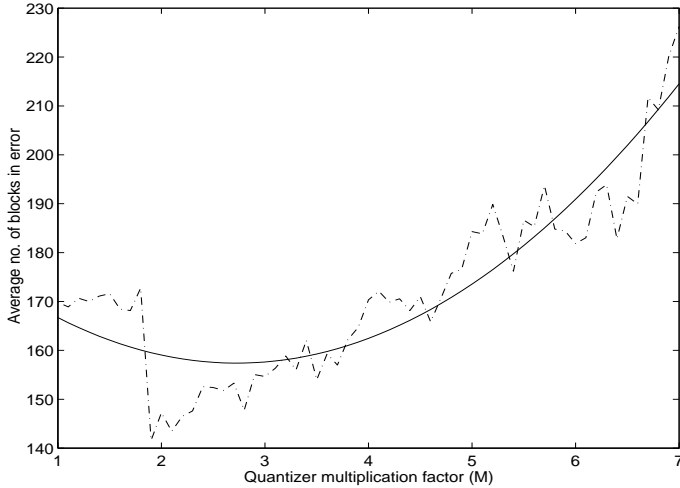


Fig. 5. Q-C curve for $p_e=10^{-3}$

p_e	M^*
10^{-1}	4.69
10^{-2}	4.71
10^{-3}	2.7
10^{-4}	2.3
10^{-5}	1

TABLE II
LOOK-UP TABLE FOR M^*

order model works well most of the time. Clearly, M^* is given by

$$\begin{aligned} M^* &= \arg \min_M B(M) \\ &= -(a_1/2a_2) \end{aligned} \quad (9)$$

The value of M^* for various p_e is given in Table II.

V. FAST ERROR RESILIENT ENTROPY CODER

We say that the error resilient encoder has *converged* when all the data bits have been packed into the slots. The number of stages for the algorithm to pack the bits is defined to be the *speed* of the algorithm. The speed of convergence of the EREC depends mainly on the efficiency of the search strategy (the offset sequence) to find an empty slot. Though the search method used in EREC is intuitively appealing and simple, it fails to exploit the statistics of the data fully. Various compression methods produce data with different statistical properties. By using this information to design the offset sequence we can design faster and better error resilient entropy coders. We propose an error resilient encoder that uses the fact that the lengths of the successive symbols (in bits) of a JPEG encoded signal are highly correlated due to the zig-zag scanning along with run length and Huffman encoders. We introduce some

terminology that will be used to describe the proposed algorithm. Let b_i , $i = 1, 2, \dots, N_1$ denote the i^{th} block of data to be placed in N_1 slots of length each equal to L . Here, N_1 corresponds to the total number of output symbols from the Huffman encoder and L is the average code length. Let $l(b_i)$ denote the number of bits in block b_i to be placed into the slots and $l(s_i^n)$ be the number of bits in slot s_i at stage n of the algorithm. The indicator function is denoted by I . In the definition given below we drop n for convenience.

Definition 1: The set $F = \{s_i, s_{i+1}, \dots, s_k\}$ is called a full cluster if $I_{\{l(s_j)=L\}} = 1$, $j = i, i+1, \dots, k$, $I_{\{l(s_{i-1})=L\}} = 0$ and $I_{\{l(s_{k+1})=L\}} = 0$.

Definition 2: The set $E = \{s_i, s_{i+1}, \dots, s_k\}$ is called a partially full cluster if $I_{\{l(s_j)=L\}} = 0$, $j = i, i+1, \dots, k$, $I_{\{l(s_{i-1})=L\}} = 1$ and $I_{\{l(s_{k+1})=L\}} = 1$.

The output blocks of the JPEG source coder whose length exceeds L are more likely to be followed by similar blocks. Likewise, blocks of size less than the average length will precede blocks of the same nature. The initial stage of FEREC is similar to EREC. Therefore, $I_{\{l(b_i) \geq L\}} = 1$ implies $I_{\{l(s_i)=L\}} = 1$ immediately after the first stage. Since consecutive blocks have similar lengths, the probability of block b_i finding a partially full slot s_j is high for $j > i+1$ when $l(b_i) \geq L$. Therefore, the block has to cross the full cluster and reach the partially full cluster in the successive stages to be placed in a slot. If F_1, F_2, \dots, F_m denote the m full clusters, then the average length of a full cluster is given by

$$L_f = \left\lceil \frac{1}{m} [\mathcal{C}(F_1) + \mathcal{C}(F_2), \dots + \mathcal{C}(F_m)] \right\rceil \quad (10)$$

and for r partially full cluster it is equal to

$$L_e = \left\lceil \frac{1}{r} [\mathcal{C}(E_1) + \mathcal{C}(E_2), \dots + \mathcal{C}(E_r)] \right\rceil \quad (11)$$

where, \mathcal{C} denotes the cardinality of a set and $\lceil \cdot \rceil$ is the ceiling function. On an average a block crosses $\lceil (L_f + L_e)/2 \rceil$ slots to find a free slot. This suggests that a better initial offset, ϕ_1 equal to $\lceil (L_f + L_e)/2 \rceil$ should speed up the packing of the data bits into the slots. Since, among the deterministic offset schemes the bi-directional search is found to be better in [19], we use a variation of it for the successive stages. In particular, the offset for the successive stages is given by

$$\phi_n = \begin{cases} -\phi_1, & \text{if } n = 2 \\ \phi_1 + (2k-1) \pmod{N_1} & \text{if } n = 2k+1 \\ \phi_1 - (2k-1) \pmod{N_1} & \text{if } n = 2k+2 \end{cases} \quad (12)$$

for $k = 1, 2, \dots$. The algorithm can be described as follows

```

for i=1 to  $N_1$ 
  /* Initialize lengths of slots */
  length( $s_i^0$ )= $L$ 
endfor
n = 1
for i= 1 to  $N_1$ 

```

```

/* Compute number of bits in  $s_i$  */
 $k_i = \min(l(b_i), [L])$ 
/* Place  $b_i$  in  $s_i$  at stage  $n$  */
 $s_i^n(1 : k_i) = b_i(1 : k_i)$ 
endfor
for i= 1 to  $N_1$ 
/* No. of bits in  $b_i$  remaining to be placed */
 $r_i = l(b_i) - [L]$ 
endfor
repeat
/* Increment stage number */
 $n = n + 1$ 
for i= 1 to  $N_1$ 
if  $r_i > 0$ 
if  $([L] - k_{i+\phi_n}) > 0$ 
temp =  $\min([L] - k_{i+\phi_n}, r_i)$ 
 $s_{i+\phi_n}^n(k_{i+\phi_n} + 1 : k_{i+\phi_n} + \text{temp}) =$ 
 $b_i(l(b_i) - r_i + 1 : l(b_i) - r_i + \text{temp})$ 
/* Update the number of bits in  $b_i$  remaining
to be placed */
 $r_i = r_i - \text{temp}$ 
/* Update the number of bits in  $s_{i+\phi_n}$  */
 $k_{i+\phi_n} = k_{i+\phi_n} + \text{temp}$ 
endif
endif
endfor
until  $r_i \leq 0, \forall i = 1, 2, \dots, N_1$ 

```

The algorithm arranges the blocks such that an error propagation does not affect the most significant bits of other blocks. This is especially important in the case of the JPEG encoder, where, the most significant bits carry more information than the least significant bits. To understand how the FEREC algorithm prevents the error propagation from affecting the most significant bits, let us consider the decoding of the slots into their respective blocks after a noisy transmission. Both the encoder and the decoder are assumed to know the values of the total number of FEREC slots N_1 , the length of each slot and the total number of transmitted bits. The decoding is done until the end of a block is reached. If a bit in a block gets corrupted it is possible that the end of the block is not detected. This means that the least significant bits of other blocks can be treated as a part of the current block. Hence, any error that occurs in a particular block affects only the least significant bits of the other block but not the most significant bit.

An Example

The working of FEREC is explained using an example. We map a set of 8 blocks of length 11, 9, 4, 3, 9, 12, 6, 2 bits respectively onto the 8 slots of size equal to 7 bits each using FEREC. The full clusters are {11, 9} and {9, 12} and the partially full clusters are {4, 3} and {6, 2}. This gives $L_f = L_e = 2$. Therefore, the initial offset is equal to 2.

The various stages of the algorithm is shown in Fig. 6. The search for empty slots is done using successive offsets equal to 0, 2, -2, 3, -1. The offset 0 corresponds to the

initial mapping of the blocks onto the slots.

VI. SIMULATION RESULTS

Simulations were done using fifty 256×256 8-bit gray level images that were compressed using the baseline JPEG in order to compare the speed and error resilience of EREC and FEREC. The images are given in [22]. The image sub-block size was chosen to be 8 for encoding. The Huffman encoded data was re-organized using FEREC before transmission. The fading channel simulator described in section III was used for the experiments. For each bit error rate, the parameters of the simulator were computed and the Rayleigh fading envelope was generated. A transmission rate of 64 kb/s was considered. A carrier frequency of 2 GHz and a Doppler frequency of 2 Hz was used to simulate the slow, non-frequency selective Rayleigh fading channel. We further assume that the values of the total number of FEREC slots, N_1 , the length of each slot and the total number of transmitted bits is sent to the decoder as protected header information. Table II was assumed to be known to both the encoder and the decoder. No post-processing was done on the received image to mitigate the effect of channel errors. Depending on the feedback from the receiver regarding the channel conditions the transmitter adaptively chose the optimal quantizer using Table II to enhance the error resilience capability. In [19] a random offset sequence is shown to converge faster than the bi-directional and uni-directional search sequence. We observed a similar behaviour with FEREC. Without loss of generality, we used the bi-directional offsets for our comparisons since the main difference between EREC and FEREC is in the initial offset computation. Channel bit error rates ranging from 10^{-4} to 10^{-1} were considered. Fig. 7 shows the original image for which the results are reported.



Fig. 7. Original image-”House”

A. Performance of adaptive quantization

Fig. 8-Fig. 10 show the reconstructed image with ($M \neq 1$) and without ($M = 1$) adaptive quantization. The proposed optimal quantizer multiplication factor (QMF)

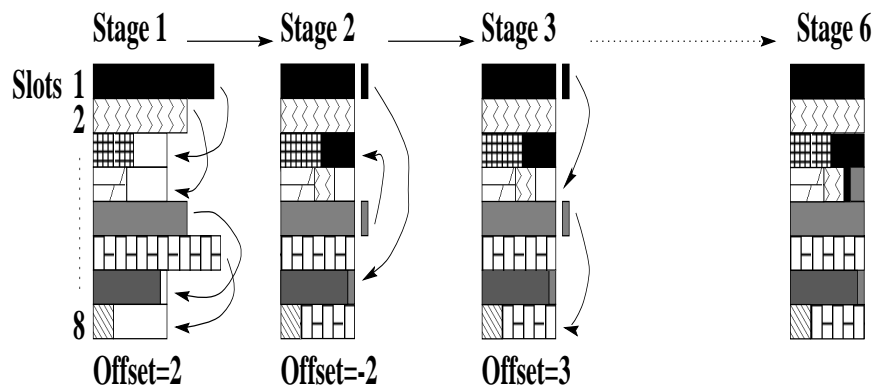


Fig. 6. An example of FEREC



Image Quantized with QMF = 1.0



Image Quantized with QMF = 4.7

Fig. 8. Reconstructed images when $p_e = 10^{-2}$



Image quantized with QMF=1.0



Image quantized with QMF=2.7

Fig. 9. Reconstructed images when $p_e = 10^{-3}$



Image quantized with QMF=1.0



Image quantized with QMF=2.3

Fig. 10. Reconstructed images when $p_e = 10^{-4}$

matched to p_e is observed to result in a better performance than a fixed quantizer. Both the visual quality and the received PSNR is higher than fixed quantization. A similar trend is observed for other bit error rates also.

B. Speed-up of FEREC over EREC

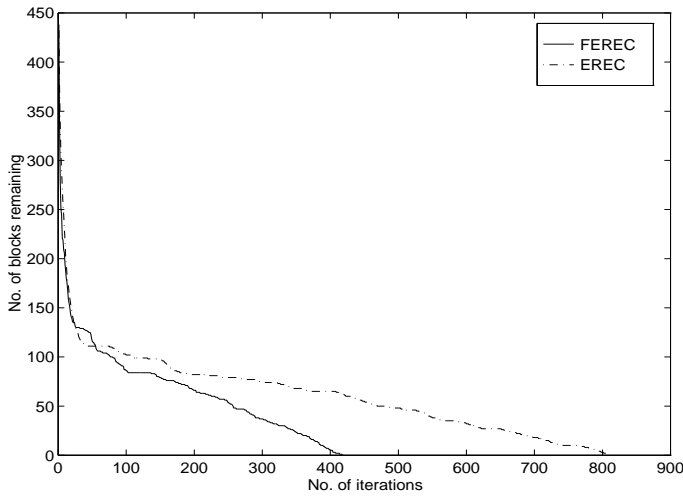


Fig. 11. Number of iterations for EREC and FEREC

The speed-up of FEREC over EREC is defined as

$$\text{Speed-up} = \frac{\text{No. of iterations for EREC to converge}}{\text{No. of iterations for FEREC to converge}} \quad (13)$$

The decrease in the number of unplaced data blocks with the iteration number is shown in Fig. 11 for the "House" image. FEREC is observed to converge in nearly half the number of iterations when compared to EREC. Therefore, the error resilient property of FEREC is expected to be

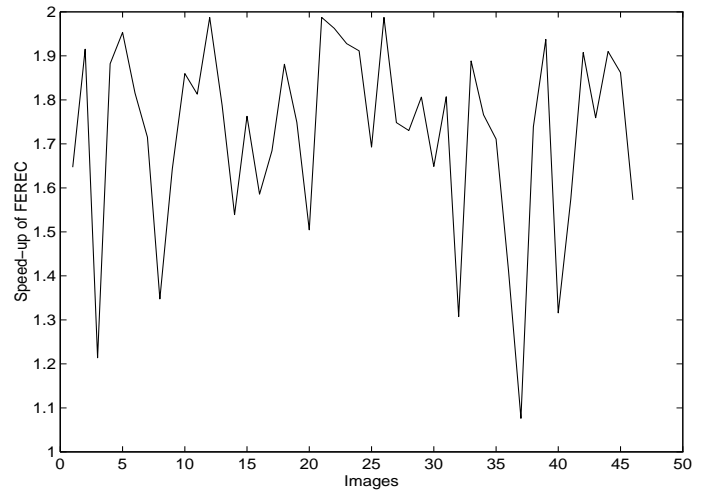


Fig. 12. Speed-up of FEREC over EREC for 50 images

better than EREC. We find that this is true as discussed later. The speed-up of FEREC for fifty images is shown in Fig. 12. It is observed to be nearly 2 for most of the images. The images corresponding to the numbers are given in [22]. This speed-up is achieved due to the search strategy that avoids searching the slots which are more likely to have been filled by other blocks in the previous iterations. We note that there could be a decrease in the speed-up when the data lengths are not sufficiently correlated. However, the output of the JPEG coder has a significant amount of correlation. Therefore, we almost always gain due to FEREC.

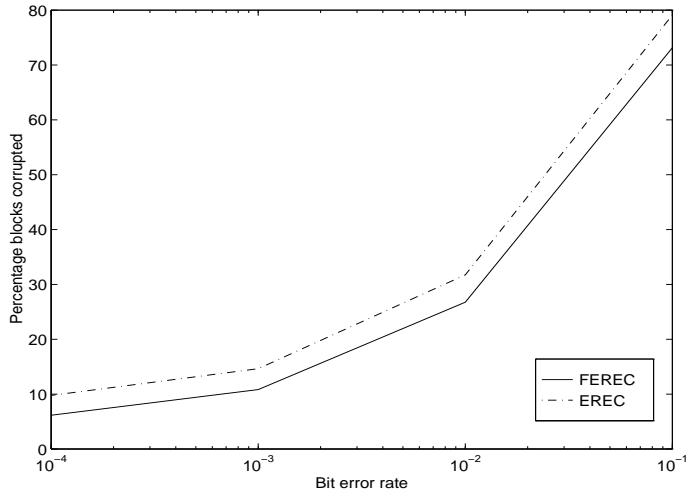


Fig. 13. Percentage blocks corrupted for EREC and FEREK

C. Percentage of significant corruption

The percentage of significantly corrupted received image sub-blocks is an important measure of comparison. A sub-block is said to be significantly corrupted if its PSNR is less than 40 dB. The threshold is set to 40 dB because this corresponds to a good visual quality. Fig. 13 shows the percentage of significantly corrupted sub-blocks for the "House" image for various channel bit error rates. FEREK is observed to outperform EREC.

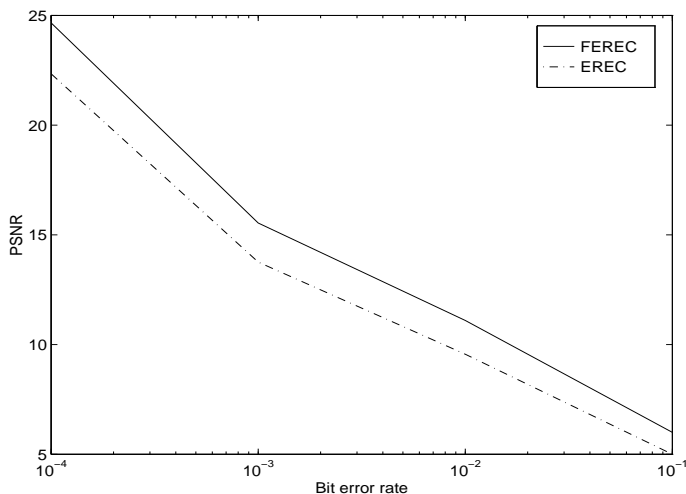


Fig. 14. PSNR without adaptive quantization for EREC and FEREK

D. Peak SNR and bit error rate

The peak SNR of the received image using EREC and FEREK is shown in Fig. 14 and Fig. 15. The results are compared in the absence and the presence of adaptive quantization. Both the algorithms exhibit similar trend

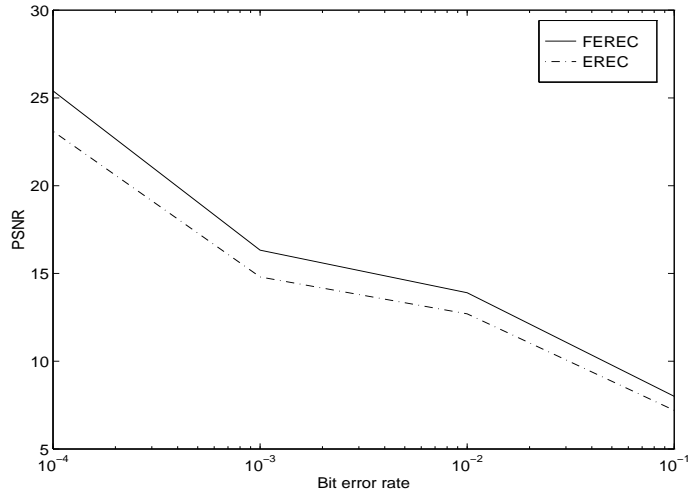


Fig. 15. PSNR with adaptive quantization for EREC and FEREK

with the adaptive quantizer resulting in a higher PSNR. FEREK consistently gives a higher PSNR than EREC for both the cases. Though PSNR alone does not truly reflect the visual quality, when combined with the percentage of significantly corrupted blocks it throws enough light on the performance of these algorithms.

VII. CONCLUSIONS

An adaptive quantizer for JPEG compressed image transmission in a slow, frequency non-selective Rayleigh fading channel is presented. The quantizer design incorporates the source and the channel characteristics using the Q-C curves. A fast error resilient coding technique that exploits the JPEG compressed source statistics is proposed. It is shown that it performs better than the EREC algorithm in terms of the speed of its convergence and error resilience. The average speed-up of FEREK is nearly two over a set of fifty images. On an average, a 5% decrease in the number of significantly corrupted blocks is also observed. The improvement in the peak SNR of the received image is upto 2 dB when compared to EREC. Modifications of the method that take into account the characteristics of compressed video is an interesting problem to study.

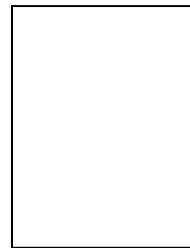
ACKNOWLEDGMENTS

The authors wish to acknowledge the anonymous reviewers for their comments and suggestions that helped in improving the presentation of the paper.

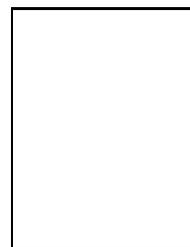
REFERENCES

- [1] A.J. Viterbi and J.K. Omura, *Principles of Digital Communications and Coding*, NY: McGraw-Hill 1979.
- [2] J.W. Modestino, D. Daut and A.L. Vickers, "Combined source channel coding of images over the block cosine transform", *IEEE Trans. on Communications*, vol. 29, pp. 1262-1274, Sept. 1981.
- [3] A. Kurtenbach and P. Wintz, "Quantization for noisy channels", *IEEE Trans. on Communication Tech.*, vol. 17, pp. 291-302, April 1969.

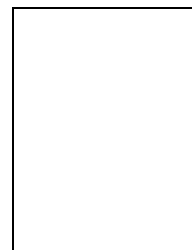
- [4] O.R. Mitchell and A.J. Tabatabai, "Channel error recovery for transform image coding", *IEEE Trans. on Communications*, vol. 29, pp. 1754-1762, Dec. 1981.
- [5] Y.Q. Zhang, Y.J. Liu and R.L. Pickholtz, "Layered image transmission over cellular radio channels", *IEEE Trans. on Vehicular Technology*, vol. 43, pp. 786-796, Aug. 1994.
- [6] P.P. Gandhi, W.E. Darlington and H.L. Dyckman, "Error-resilient image compression based on JPEG", *Proceedings of the SPIE*, vol. 2669, pp. 106-123.
- [7] E.S. Jang and N.M. Nasrabadi, "Subband coding with multi-stage VQ for wireless image communication", *IEEE Trans. on Circuits and Systems for Video Tech.*, vol. 5, pp. 247-253, June 1995.
- [8] L. Hanzo and J. Streit, "Adaptive low-rate wireless videophone schemes", *IEEE Trans. on Circuits and Systems for Video Tech.*, vol. 5, pp. 305-318, Aug. 1995.
- [9] T.J. Ferguson and J.H. Rabinowitz, "Self-synchronizing Huffman codes", *IEEE Trans. on Information Theory*, vol. 30, pp. 687-693, July 1984.
- [10] N. MacDonald, "Transmission of compressed video over radio links", *SPIE Visual Commun. Image Processing*, pp. 1484-1488, 1992.
- [11] D.W. Redmill, "Robust architectures for image and video coding", *2nd International Workshop on Mobile Multimedia Communications*, Apr. 1995.
- [12] W.M.Lam and A.R. Reibman, "Self-synchronization variable-length codes for image transmission", *Proc. Intl. Conf. on Acoustics, Speech and Signal Proc.*, vol. III, pp. 477-480, 1992.
- [13] T. Kawahara and S. Adachi, "Video transmission technology with effective error protection and tough synchronization for wireless channels", *Proc. of Intl. Conf. on Image Processing*, vol. 2, pp. 101-104, 1996.
- [14] K. Sayood and J.C. Borkenhagen, "Use of residual redundancy in the design of joint source/channel coders", *IEEE Trans. on Communications*, vol. 39, pp. 838-846, June 1991.
- [15] W.J. Zeng and Y.F. Huang, "Boundary matching detection for recovering erroneously received VQ indices over noisy channels", *IEEE Trans. on Circuits and Systems for Video Tech.*, vol. 6, pp. 108-113, Feb. 1996.
- [16] Q. Zhu, Y. Wang and L. Shaw, "Coding and cell-loss recovery in DCT-based packet video", *IEEE Trans. on Circuits and Systems for Video Tech.*, vol. 3, pp. 248-258, June 1993.
- [17] R. Stedman, H. Gharavi, L. Hanzo and R. Steele, "Transmission of subband-coded images via mobile channels", *IEEE Trans. of Circuits and Systems for Video Tech.*, pp. 15-26, Feb.1993.
- [18] M. Khansari, A. Jalali, E. Dubois and P. Mermelstein, "Low bit-rate video transmission over fading channels for wireless microcellular systems", *IEEE Trans. on Video Tech.*, vol. 6, pp. 1-11, Feb. 1996.
- [19] N.T. Cheng and N.G. Kingsbury, "The ERPC: An efficient error-resilient technique for encoding positional information on sparse data", *IEEE Trans. on Communications*, vol. 40, pp. 140-148, Jan. 1992.
- [20] D.W. Redmill and N.G. Kingsbury, "The EREC: An error resilient technique for coding variable-length blocks of data", *IEEE Trans. on Image Processing*, vol. 5, pp. 565-574, April 1996.
- [21] W.B. Pennebaker and J.L. Mitchell, *JPEG: Still image data compression standard*, NY: International Thomson Publishing, 1993.
- [22] S.J. Ramadoss, *Adaptive quantization and fast error resilient entropy coding for using JPEG in wireless communication*, M.S. Thesis, University of South Florida, 1996.
- [23] K. Pahlavan and A.H. Levesque, *Wireless Information Networks*, John Wiley & Sons, 1995.
- [24] N.S. Jayant and P. Noll, *Digital Coding of Waveforms, Principles and Applications to Speech and Video*, Englewood Cliffs, NJ: Prentice-Hall Inc, 1984.



R Chandramouli is currently a Ph.D candidate in the Department of Computer Science and Engineering at the University of South Florida, Tampa. He received his BSc in Mathematics from Loyola College, University of Madras, India and M.E. in ECE from the Indian Institute of Science, Bangalore in 1990 and 1994 respectively. He was a software engineer in the DSP group of Motorola, India and a Junior Research Fellow in the Department of Mathematics, Statistics, and Computing Science, University of New England, Australia from 1994-'95. He has received the IEEE Computer Society Richard E. Merwin Scholarship, 1997, Australian Research Council Fellowship, 1995, and Sri. Raghavendra Merit Scholarship for Mathematics in 1988. His research interests include statistical communication theory, wireless communications, image and video compression, and low power/reliability issues in VLSI.



N Ranganathan is currently an associate professor in the Department of Computer Science and Engineering and the Center for Microelectronics Research at the University of South Florida, Tampa. He received his Ph.D in Computer Science from the University of Central Florida in 1988. His research interests include VLSI design and hardware algorithms, computer architecture and parallel processing. He has published widely in reputed journals and conferences and holds five U.S patents. Dr. Ranganathan is a Senior Member of IEEE, member of IEEE Computer Society, IEEE CS Technical Committee on VLSI, ACM and VLSI Society of India. He served as the Program Co-Chair for VLSI Design'94 and as the General Co-Chair for VLSI Design'95 and VLSI Design'98. He has served on the program committees of international conferences such as ICCD, ICPP, IPPS, SPDP, VLSI Design, GLSVLSI and ICHPC. Currently, he serves as an Associate Editor of the IEEE Transactions on CSVT, the IEEE Transaction on Circuits and Systems (TCAS-II), Pattern Recognition and the International Journal on VLSI Design. He guest edited a special issue of International Journal of Pattern Recognition and Artificial Intelligence on VLSI for PR and AI published in April 1995. He is the editor of a two-volume series titled VLSI Algorithms and Architectures published by IEEECS Press in June 1993. Recently, he has been elected as the Chair of the IEEE Computer Society Technical Committee on VLSI for the term 1998-2000.



Shivaraman J Ramadoss is currently working as a Research Engineer with Digital Video Express, Lp. He received his M.S. in Computer Engineering from USF, Tampa in Dec. 1996 and B.E. from SVCE, University of Madras in 1994. He was with Dynacs Eng. Co. as a Software Engineer from 1994-1997 developing applications in the field of aerospace simulation and modeling. He is a member of the honor society of Phi Kappa Phi. His research interests are in the areas of Digital Image Processing and Video Compression.